Purchased Power Dispatching Potential Evaluation of Steel Plant With Joint Multienergy System and Production Process Optimization

Lei Gan, *Member, IEEE*, Tianyu Yang, Xingying Chen, *Senior Member, IEEE*, Gengyin Li, *Member, IEEE*, and Kun Yu, *Member, IEEE*

***Abstract*—Iron and steel industry is the pillar industry of China, providing a solid foundation for China's industrialization. While steel plants are energy intensive mainly consuming coal and electricity, and their power consumption tends to be higher proportional in the near future, due to global confidence of peak and neutrality carbon dioxide emission, electrical substitution, and ongoing energy use right transaction. Thus, these plants will have larger potential to participate in the friendly interaction between power supply and demand. The adjustable potential of purchased power load exists in two aspects: one is the controllable resources of inner energy supply and use system, and the other is the energy schedule regulation accompanied by production process adjustment, which is rarely considered in current energy management research of steel plants. Based on the flexibility analysis of production process control without affecting productivity, the adjustment model of steel-rolling lines, air separation and electric arc furnaces on iron-making line is formulated here, as well as the corresponding energy consumed in these processes. Combined with the optimization of multienergy coupling system and production processes, a joint evaluation model of maximum dispatching potential and duration is proposed and solved by mixed-integer linear programming solver. Simulation result shows the feasibility of the proposed dispatching potential evaluation method and the effectiveness to take the production process adjustment with energy-system scheduling.**

***Index Terms*—Dispatching potential, iron and steel plant (ISP), multienergy coupling system, production process optimization.**

Manuscript received October 23, 2021; revised December 11, 2021; accepted January 14, 2022. Date of publication January 25, 2022; date of current version March 20, 2022. Paper 2021-PSEC-1307.R1, presented at the 2021 IEEE/IAS Industrial and Commercial Power System Asia (I&CPS Asia), Chengdu, China, Jul. 18–21, 2021, and approved for publication in the IEEE TRANSACTIONS ON INDUSTRY APPLICATIONS by the Power Systems Engineering Committee of the IEEE Industry Applications Society. This work was supported in part by the Key R&D plan of Jiangsu Province under Grant BE2020688 and in part by the State Key Laboratory of Alternate Electrical Power System with Renewable Energy Sources under Grant LAPS21003. *(Corresponding author: Lei Gan.)*

Lei Gan, Tianyu Yang, Xingying Chen, and Kun Yu are with the College of Energy and Electrical Engineering, Hohai University, Nanjing 211100, China (e-mail: leigan@hhu.edu.cn; tianyu_yang_hhu@163.com; xychen@hhu.edu.cn; kun.yu@vip.sina.com).

Gengyin Li is with the State Key Laboratory of Alternate Electrical Power System With Renewable Energy Sources, North China Electric Power University, Beijing 102206, P. R. China (e-mail: ligy@ncepu.edu.cn).

Color versions of one or more figures in this article are available at https://doi.org/10.1109/TIA.2022.3144652.

Digital Object Identifier 10.1109/TIA.2022.3144652

Nomenclature

A. Subscripts

i	Index of by-product coal gas type, $i = 1, 2, 3$.
j	Index of steam boilers and generator, $j = 1, 2, 3, \ldots, J$; J is the number of steam boilers.
t	Index of time periods, $t = 1, 2, 3, \ldots, T$; T is the number of time periods.
n	Index of electric arc furnaces, $n = 1, 2, 3, \ldots, N$, where N is the number of electric arc furnaces.
k	Index of electric arc furnace operating cycles, $k = 1, 2, 3, \ldots, K$; K is the number of operating cycles.

B. Main Variables

$V_{i,t}^{\mathrm{gas}}$	Gas holder reserve of gas type i.
$\Delta V_{i,t}^{\mathrm{gas}}$	Reserve change of gas type i.
V_t^{oxy}, V_t^{nit}	Reserves of oxygen (nitrogen) holder.
$\Delta V_t^{\mathrm{oxy}}$, $\Delta V_t^{\mathrm{nit}}$	Reserve change of oxygen (nitrogen).
$f_{i,t}^{\mathrm{roll,gas}}$	Flow rate of gas i consumed in rolling production.
$f_{i,j,t}^{\mathrm{gas}}$	Input gas flow rate of gas i in boiler j.
$f_{j,t}^{\mathrm{steam}}$	Output steam flow rate of boiler j.
$f_{j,t}^{\mathrm{water}}$	Input water flow rate of boiler j.
$f_{j,t}^{\mathrm{gen,steam}}$	Input steam flow rate to power generator j from boiler j.
$f_{j,t}^{\mathrm{steam,release}}$	Flow rate of steam released from boiler j.
$f_t^{\mathrm{roll,steam}}$	Steam consumed rate in steel rolling.
$f_t^{\mathrm{other,steam}}$	Steam consumed rate in other production processes.
P_t^{gas}	Total power of byproduct gas generation.
$P_{j,t}^{\mathrm{gen,gas}}$	Output power of steam generator j consuming by-product gases.
P_t^{oxy}, P_t^{nit}	Power consumed to produce oxygen (nitrogen).
P_t^{roll}	Power consumed in steel rolling line.
P_t^{grid}	Purchased power from power grid.
P_t^{change}	Difference between base and optimized load, i.e., dispatching potential of purchased load.
$n_{i,j,t}$	Inlet valve opening for gas i to boiler j.
x_t	Binary variable representing the operational state of rolling line.

$\xi_{n,t}$	Binary variable to determine whether electric arc furnace *n* is experiencing operating cycle.

C. Parameters

$V_{i,t}^{\mathrm{gas,min}}$	Minimum reserve of gas holder *i*.
$V_{i,t}^{\mathrm{gas,max}}$.	Maximum reserve of gas holder *i*.
$\Delta V_{i,t}^{\mathrm{gas,max}}$	Maximum reserve change of gas *i*.
$f_{i,t}^{\mathrm{pro,gas}}$	Gas production of gas type *i*.
$f_{i,t}^{\mathrm{other,gas}}$	Demand for gas *i* in other fixed production processes.
$f_{t}^{\mathrm{oxy,dem}}$	Oxygen demand consumed in production.
$f_{t}^{\mathrm{nit,dem}}$	Nitrogen demand consumed in production.
$P_{t}^{\mathrm{gen,heat}}$	Output power of CDQ at time *t*.
$P_{t}^{\mathrm{gen,PV}}$	Output power of PV at time *t*.
$P_{t}^{\mathrm{grid,base}}$	Baseline purchased power without optimization.
P_{t}^{other}	Nonadjustable power demand of steel plant.
p^{oxy}	Electricity demand to produce 1 m^3 oxygen.
p^{nit}	Electricity demand to produce 1 m^3 nitrogen.
H_i	Enthalpy of gas type *i*.
$H_{j,t}^{\Delta}$	Enthalpy of mixed gas in boiler *j*.
$H_{j,t}^{\mathrm{steam}}$	Enthalpy of output steam in boiler *j*.
$H_{j,t}^{\mathrm{water}}$	Enthalpy of input water in boiler *j*.
$L_{i,j}$	Designed maximum flow rate of gas pipe for gas *i* to boiler *j*.
$\eta_{j}^{\mathrm{steam}}$	Efficiency of steam boiler *j*.
η_{t}^{tb}	Constant energy conversion efficiency.
$\eta^{\mathrm{CDQ,steam}}$	Proportionality coefficient of CDQ.
m_t	Amount of CDQ.
E_t	Solar illumination.
T_fur	Number of time periods in an electric arc furnace operating cycle.
T^{DR}	Dispatching time set for specific demand response project.
Δt	Time interval of dispatching.
ΔT^{dur}	Duration of dispatching potential.

I. Introduction

WITH the proposal of China's carbon emission target to achieve carbon peak and neutrality by 2030 and 2060, electrical substitution will be implemented at energy consumption side, leading to the power demand explosion in future. At the same time, with the mainstream to exploit intermittent clean power instead of fossil fuel, the contradiction between power supply and demand will be more severe. The potential exploitation of adjustable resources on the power demand side can mitigate supply tension, realizing friendly supply-demand interaction through demand response projects. As one of the pillar industries of China's heavy industry, the power consumption of iron and steel industry will also grow rapidly, representing larger dispatching potential to participate in demand side management for steel plants.

On the perspective of energy system in iron and steel plants (ISPs), a large amount of by-product coal gas can be produced and consumed in different production processes with primary energy input including purchased electricity and coal/coke. As an important secondary energy source in plant production, by-product gas accounts for about 30% of plant energy consumption [1]. At the same time, the steam produced in the production process also occupies a certain proportion in the energy consumption. Thus, the energy system in a steel plant is highly coupled with multiple energy forms including electricity, by-product gas, and steam. Therefore, multienergy coupling analysis is vital to the energy optimization scheduling. Practice shows that reasonable scheduling of by-product gas and intermediate heating steam can effectively reduce power load of an ISP, restrain the load fluctuation, improve the safety of power grid operation, achieve energy conservation, and emissions reduction. At present, related scholars have done a lot of research on multienergy coupling and its optimal scheduling in iron and steel industry. The authors in [2] proposed an energy scheduling method to minimize the overall operation energy cost of a power plant considering by-product gas and steam. The authors in [3] studied the operation scheduling problem of the medium and low pressure steam system with the steam conversion constraints taking different pressure level into account. The authors in [4] established a by-product gas and steam scheduling model considering the cost of pollutant emission, realizing synchronous improvement of economic benefits and environmental benefits. Owned power plant with primary energy of by-product gas was studied in [5]. The influence of boiler inlet design on by-product gas power generation is discussed in [6]. Energy scheduling methods in [7] and [8] discussed the influence on production and by-product gas power generation caused by the gas position of gas holder and the efficiency change of steam turbine under different loads. The authors in [9] proposed a novel data-driven real-time predictive optimization method to schedule the dispatch of by-product gas system based on SCADA system of steel plant. With a utility function introduced in the critic network considering the time delay of the Linz-Donawitz Process gas (LDG) system, a scheduling method to meet the demand of LDG system was realized in [10] based on modified evolutionary algorithm. A regression model of gas consumption and output of each furnace is established in [11], to achieve the highest production efficiency and lowest production cost by distributing the byproduct gas and purchased natural gas reasonably among the furnaces. As shown in the above, the energy system scheduling of a steel plant is complex with power, heterogeneous by-product gas, and steam coupled tightly. Thus, to realize the interaction between the energy intensive steel plants with power grid, it is necessary to study on the coupling of the multienergy system in dispatching potential evaluation of outsourcing electric power. Our previous work proposed an optimization method to evaluate steel plants' dispatching potential considering multi-energy coupling system [12]. However, all of the above research work has a same hypothesis with constant production processes to assure the productivity.

Practically, the schedule of different production processes in a steel plant can also be adjusted to save energy cost without affecting productivity according to the energy price signals or demand side incentives. Current research has shown the great regulation flexibility in different production processes. A two-stage genetic algorithm was proposed to optimize the scheduling of steel-making and continuous casting process, realizing the reduction of process time [13]. The authors in [14] studied the adjustable running speed of continuous casting process equipment to further reduce the energy consumption. The authors in [15] studied the optimization scheduling of hot rolling process based on demand response, and realized the multiscale energy saving of hot rolling process. The authors in [16] studied the configuration of air separation equipment in ISPs, and the load optimization is made use of the load translation characteristic of it. A bi-level soft decision scheduling was proposed to reduce the consuming time of continuous casting process considering continuous casting process failure; the waste of time in continuous casting process is reduced through the optimization [17]. Similarly, a bi-level programming genetic algorithm was applied to efficient scheduling of steelmaking process [18]. In order to meet production and investment needs of enterprises, and maximize economic benefits, [19] studies how to use TOU power price and typical scene extraction to model for coordinating short-term and long-term planning of power intensive enterprises. The authors in [20] list a variety of emerging technologies that can reduce energy consumption and carbon dioxide emissions in iron making process, providing a basis for subsequent research. The authors in [21] present an overview of different steel production routes, including the blast furnace-basic oxygen furnace(BF-BOF) route, the electric arc furnace (EAF) route, and the combination of them. And the status quo of the material and energy flows of the iron and steel industry was presented. The production scheduling problem of iron and steel enterprises under multiple power access channels was studied in [22], and the economic benefit is improved through joint optimization of production plan and electricity cost. A nonlinear programming model for oxygen system scheduling was proposed in [23] to restrict the practical adjusting capacity, fill the imbalance gap of oxygen, and minimize the electricity cost. A multiobjective energy and raw material consumption of electric arc furnaces were scheduled by nondominated sorting genetic algorithm II [24].

As we can see, flexible control is suitable in many production processes without affecting productivity, such as air separation system control, steel making, casting, and rolling processes. Along with the adjustable process, the related consuming energy can be regulated, contributing to greater dispatching potential of multienergy system. Therefore, the in-depth study on the optimization of high energy-consumption production processes can also achieve energy cost saving and friendly interaction with the external energy supply system.

To the best of our knowledge, current research about the scheduling of ISPs has carried out in-depth studies on single-energy optimization, multienergy coupling management, and adjustment of different production processes for energy saving, demand response, or other targets separately. However, few studies payed attention on the joint dispatch of energy and production process comprehensively, contributing to greater potential of demand response. Based on the analysis on the adjustable inner multienergy coupling system and production possesses of a typical ISP and our previous research [25], a mixed-integer linear programming (MILP) model was formulated and solved to evaluate the dispatching potential of purchased power load in this article.

The main contributions can be listed as follows.

1) Complex multienergy system of a typical ISP is modeled based on the analysis on energy supply and use structure with inner power, steam, and by-product coal gas system coupled with each other.
2) The energy consumption of adjustable production processes is analyzed and formulated according to their operational constraints, mainly including interruptible steel rolling process, transferrable air separation, and electric arc furnace operation of steel-making processes.
3) Two dimensions of purchased power dispatching potential evaluation, maximum value, and its duration, were formulated as a mix-integer linear programming model coordinating energy system and product process adjustment, solved by CPLEX solver. Numerical shows the necessity to combine energy system and production process together to obtain greater dispatching potential.

II. Modeling of Multienergy System

A. Structure of Inner Multienergy Coupling System

Inside a typical ISP, its power system, thermal system, and by-product coal gas system are complicatedly coupled with each other on both the inner energy supply side and energy consumed side along with different production processes. To study on the dispatching potential of outsourcing electric power, the modeling of inner multienergy system should be conducted first, shown in Fig. 1.

At present, the typical steel production process includes sintering, coking, pelletizing, ironmaking, steelmaking, rolling, and other processes. Among them, sintering, coking, pelletizing, and other processes are used to produce mineral raw materials and fuels (such as coke) for the main processes such as ironmaking. The impurities of processed iron ore are removed by iron-making and steelmaking processes. In the traditional steel production, converter steelmaking process is generally adopted. With the upgrading of technology, steel enterprises replace converter steelmaking with electric arc furnace to reduce energy consumption gradually. After steel making, the treated molten steel is rolled into different types according to product demand. At the same time, iron and steel production also includes various auxiliary processes, such as oxygen and nitrogen production by air separation system, dust removal fan, water supply, etc.

As we can see, primary input energy to an ISP mainly includes coking coal, electricity purchased from external power grid, and generated by distributed photovoltaic panels (PV). Intermediate energy produced and consumed inside an ISP mainly includes by-product gases, electricity generated by owned thermal power plant (TPP), steam, and waste heat. By-product gas combustion and waste heat from main production processes are the main resources to drive steam turbine generators of owned TPP. There are three kinds of intermediate by-product coal gas involved in ISPs, namely coke oven gas (COG), blast furnace gas (BFG), and LDG produced in the process of coking, ironmaking, and steelmaking, respectively. The by-product gases will be stored

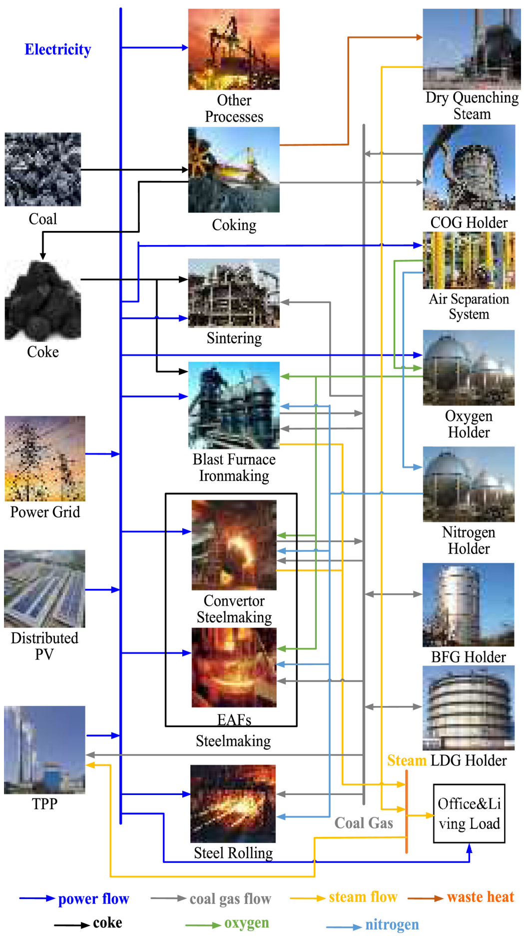

Fig. 1. Typical multienergy system inside an ISP.

in different gas holders and supplied to the main production lines and applied to power generation as required.

For energy saving and emission reduction, recovery techniques of waste heat are widely used in most of current ISPs to improve energy efficiency and economy. Coke dry quenching (CDQ) technique is widely used in modern coking process [26]. With this technique, cold inert gas is used to cool the high-temperature coke, and the heat of heated inert gas can be transferred to waste heat boiler to make steam for power generation.

B. Modeling of By-Product Gas System

Each of intermediate by-product gases (COG, BFG, and LDG) is produced, consumed, and stored in specific gas holder. The volume change of each gas holder can be defined as (1)

$$\Delta V_{i,t}^{\text{gas}} = V_{i,t}^{\text{gas}} - V_{i,t-1}^{\text{gas}} = \left(f_{i,t}^{\text{pro,gas}} - f_{i,t}^{\text{roll,gas}} - f_{i,t}^{\text{other,gas}} - \sum_{j=1}^{J} f_{i,j,t}^{\text{gas}} \right) \Delta t. \tag{1}$$

To keep operational safety, gas reserves should be kept in an appropriate position. Excessive reserves will increase the risk of gas storage, while the lack of reserves may not be able to meet the gas demand of the main processes. In order to study the dispatching potential of ISPs, this article tries to control the gas volume position without affecting production, so as to achieve more dispatching potential of purchased power load. Thus, the gas volume position of holders can be formulated as (2) and (3)

$$-\Delta V_i^{\text{gas,max}} \le \Delta V_{i,t}^{\text{gas}} \le \Delta V_i^{\text{gas,max}} \tag{2}$$

$$V_i^{\text{gas,min}} \le V_{i,t}^{\text{gas}} \le V_i^{\text{gas,max}}. \tag{3}$$

Besides, the enthalpy of mixed gas for power generation must be above the minimum standard, subjected to (4) and (5)

$$H_{j,t}^{\Delta} \sum_{i=1}^{I} f_{i,j,t}^{\text{gas}} = \sum_{i=1}^{I} (f_{i,j,t}^{\text{gas}} H_i) \tag{4}$$

$$H_{j,t}^{\Delta,\min} \le H_{j,t}^{\Delta}. \tag{5}$$

For each generator, the input gas can be controlled by the opening of inlet valves, denoted as $n_{i,j,t}$, and the regulation accuracy is 1% [6]. Thus, the constraints of ${f_{i,j,t}}^{\text{gas}}$ can be described as (6) and (7)

$$f_{i,j,t}^{\text{gas}} = n_{i,j,t} L_{i,j} \tag{6}$$

$$n_{i,j,t}^{\min} \le n_{i,j,t} \le n_{i,j,t}^{\max}. \tag{7}$$

C. Modeling of Steam System

For each steam generator, there is a mixed gas boiler to produce steam. The energy conversion relationship between the by-product gas and steam in boiler is shown in (8)

$$\eta_j^{\text{steam}} H_{j,t}^{\Delta} \sum_{i=1}^{I} f_{i,j,t}^{\text{gas}} = f_{j,t}^{\text{steam}} H_{j,t}^{\text{steam}} - f_{j,t}^{\text{water}} H_{j,t}^{\text{water}}. \tag{8}$$

The steam balance in system can be formulated as (9)

$$\sum_{j}^{J} f_{j,t}^{\text{steam}} = \sum_{j}^{J} f_{j,t}^{\text{gen,steam}} + \sum_{j}^{J} f_{j,t}^{\text{steam,release}} + f_t^{\text{roll,steam}} + f_t^{\text{other,steam}}. \tag{9}$$

The steam flow rate out from boiler was subjected to technique limitations (10)

$$f_{j,t}^{\text{steam,min}} \le f_{j,t}^{\text{steam}} \le f_{j,t}^{\text{steam,max}}. \tag{10}$$

D. Modeling of Power System

As for power system of an ISP, power sources mainly composed of purchased power, gas-steam turbines, distributed PV, and CDQ waste heat generation mentioned above.

1) Gas-Steam TPP: Generally, there are several steam turbines inside an ISP, the total output power of these turbines ${P_t}^{\text{gas}}$ can be described as

$$P_t^{\text{gas}} = \sum_{j=1}^{J} P_{j,t}^{\text{gen,gas}}. \tag{11}$$

The output power of generator j at time t can be defined as (12), and the output power of generators is constrained by its technical upper and lower limitations, shown as (13)

$$P_{j,t}^{\text{gen,gas}} = f_{j,t}^{\text{gen,steam}} H_{j,t}^{\text{steam}} \eta_j^{tb} \tag{12}$$

$$P_{j,t}^{\text{gas,min}} \leq P_{j,t}^{\text{gen,gas}} \leq P_{j,t}^{\text{gas,max}}. \tag{13}$$

2) CDQ Waste Heat Generation: The steam output of the dry quenching system is directly proportional to the amount of high-temperature coke. In this article, the proportionality coefficient is set as a constant $\eta^{\text{CDQ,steam}}$, as shown in (14). The constraints of steam power generation efficiency and steam input are shown in (15) and (16)

$$P_t^{\text{gen,heat}} = f_t^{\text{steam,dry}*} H_t^{\text{steam,dry}*} \eta^{tb,\text{dry}} \tag{14}$$

$$f_t^{\text{steam,dry}} + f_t^{\text{CDQ,release}} = \eta^{\text{CDQ,steam}*} m_t \tag{15}$$

$$f_t^{\text{steam,dry,min}} \leq f_t^{\text{steam,dry}} \leq f_t^{\text{steam,dry,max}}. \tag{16}$$

3) Photovoltaic Power Generation: The photovoltaic power generation is related to the illumination area, illumination intensity and conversion efficiency (17)

$$P_t^{\text{gen,PV}} = E_t{}^* \eta_t^{\text{PV}*} S_t^{\text{PV}}. \tag{17}$$

III. Modeling of Adjustable Production Processes

The scheduling of production processes is profit-oriented. Because of the nondominant proportion in the overall operational cost, about 25%–35%, the energy system operation is generally scheduled under the precondition to keep the productivity. According to our investigation, the production dispatching of an ISP has the adjustable potential to make the production duration shorter and energy consumption less. Thus, the optimization of production processes can contribute to the outsourcing power dispatching potential significantly. Similar to the classification of flexible power load, the adjustable characteristics of production processes can be classified into three categories: interruptible, transferrable, and reducible ones. To not affect the yield of iron and steel, three adjustable production processes are considered as follows.

A. Modeling of Interruptible Steel Rolling Production Line

According to our survey, it is found that the steel rolling production line can be shut down before 1 h-ahead notification when there are sufficient steel inventories. The interruption can be conducted once in a day and last for 1 h. The production lines can be dispatched one day ahead Therefore, the modeling of steel rolling production line in this article is based on its interruptible property. When the rolling line is interrupted, the demand for electricity, gas, and steam will be zero, which provides a lot of space for the optimal scheduling of ISPs. When the dispatching interval is set as 5 min, the interruptible load modeling can be formulated as (18)–(22)

$$P_t^{\text{roll}} = x_t{}^* P_t^{\text{roll,base}} \tag{18}$$

$$f_{i,t}^{\text{roll,gas}} = x_t{}^* f_{i,t}^{\text{roll,gas,base}} \tag{19}$$

$$f_t^{\text{roll,steam}} = x_t{}^* f_t^{\text{roll,steam,base}} \tag{20}$$

$$\sum_{t=1}^{24/\Delta t} x_t \geq (24 - T^{\text{shut}})/\Delta t \tag{21}$$

$$\sum_{u}^{u+T^{\text{shut}}/\Delta t-1} x_u = 0. \tag{22}$$

If x_t is "1," it stands for steel rolling production line is running, otherwise "0." P_t^{roll} represents the consumed power of steel rolling line; The superscript base means the symbols are parameters representing the energy consumed when the production line is running.

B. Modeling of Transferrable Air Separation System

Air separation system is an extremely important auxiliary equipment in steel production, producing oxygen, nitrogen, and other gases that are needed in each process. With separating, purifying air, and extracting these gases, the power consumption of air separation system accounts for 15%–20% of the total power consumption for an ISP [27]. With the gasholder for different gases, the air separation system becomes to be transferrable under the precondition to keep the stored gases within their safe range.

The power consumption of oxygen and nitrogen in the air separation system is proportional to the production volume, denoted as (23) and (24)

$$P_t^{\text{oxy}} = p^{\text{oxy}*} f_t^{\text{oxy}} \tag{23}$$

$$P_t^{\text{nit}} = p^{\text{nit}*} f_t^{\text{nit}}. \tag{24}$$

The volume of stored gas in oxygen carrier can be formulated as (25). Due to the constraints of gas pipeline, the changed volume of oxygen should be subjected to (26). To keep safe production, the volume of oxygen in gas holder carrier must meet (27)

$$\Delta V_t^{\text{oxy}} = V_t^{\text{oxy}} - V_{t-1}^{\text{oxy}} = (f_t^{\text{oxy}} - f_t^{\text{dem,oxy}})\Delta t \tag{25}$$

$$|\Delta V_t^{\text{oxy}}| \leq \Delta V^{\text{oxy,max}} \tag{26}$$

$$V^{\text{oxy,min}} \leq V_t^{\text{oxy}} \leq V^{\text{oxy,max}}. \tag{27}$$

Similarly, the constraints of nitrogen volume can be described as (28)–(30)

$$\Delta V_t^{\text{nit}} = V_t^{\text{nit}} - V_{t-1}^{\text{nit}} = (f_t^{\text{nit}} - f_t^{\text{dem,nit}})\Delta t \tag{28}$$

$$\left|\Delta V_t^{\text{nit}}\right| \leq \Delta V^{\text{nit,max}} \tag{29}$$

$$V^{\text{nit,min}} \leq V_t^{\text{nit}} \leq V^{\text{nit,max}}. \tag{30}$$

C. Modeling of Electric Arc Furnaces in Steel-Making Process

To realize reduction of carbon emission and electrical substitution, electric arc furnace will be a main device applied in steel-making processes. The power load of electric arc furnace to make steel is a typical impact load with high power consumption and has great impact on power grid when starting up. Mathematically, the load curve of one production period is a discontinuous step function with different fixed value [28], as shown in Fig. 2.

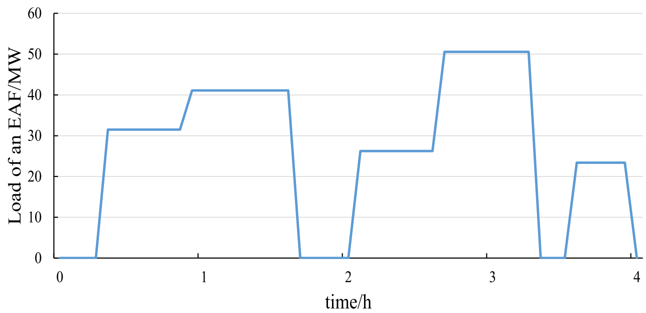

Fig. 2. Load curve of an arc furnace in one production period.

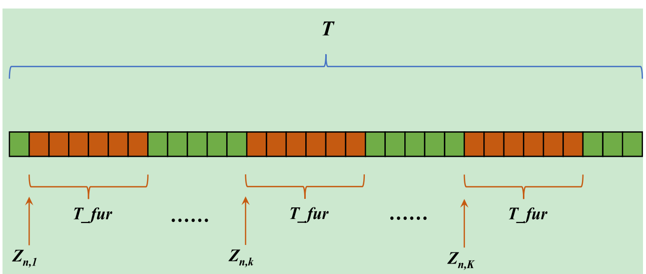

Fig. 3. Load distribution of EAF in the whole operation cycle.

Generally, an ISP has several electric arc furnaces. By dispatching the starting time of multiple electric arc furnaces, the total load of electric arc furnaces can be transferrable without affecting the productivity. During the production process, each electric arc furnace will complete a certain number of operating cycles. Therefore, the total load of the electric arc furnace in any period is shown in (31)

$$P_t^{\mathrm{fur}} = \sum_{n=1}^{N} P_{n,t}^{\mathrm{fur}}. \tag{31}$$

Where, P_t^{fur} represents the consumed power of arc furnace at moment t; subscript n is the index of arc furnace.

According to Fig. 2, the power load of each EAF within one cycle can be represented as an array where are a elements in it. (a is the number of time periods contained within a load cycle.) Each element in it is represented as P_a^{fur}. Similarly, the load of each EAF during its entire scheduling cycle can be described as an array where are T_fur elements in it, where k (1, 2, 3, …, K) is the number of operating cycle. The starting time of each operating cycle of electric arc furnace is described as $z_{n,k}$. Thus, the load of each EAF in any time period can be determined if $z_{n,k}$ is determined, denoted as (32) and Fig. 3

$$\begin{cases} P_{n,(z_{n,k}+a-1)}^{\mathrm{fur}} = P_a^{\mathrm{fur}} \quad \forall a = 1, 2, 3, \ldots, T\_\mathrm{fur} \\ \xi_{n,t} = 1 \quad \forall t \in [z_{n,k}, z_{n,k} + T\_\mathrm{fur} - 1] \\ \sum_{t=1}^{T} \xi_{n,t} = T\_\mathrm{fur}^{*} K \\ P_{n,t}^{fur} = \xi_{n,t}{}^{*} P_{n,t}^{fur} \end{cases}. \tag{32}$$

To ensure the integrity of the EAF producing cycle, the starting time of each cycle should not be earlier than the end time of the previous cycle, and the starting time of the last cycle should ensure that the last cycle can run completely, denoted as(33)

$$\begin{aligned} z_{n,k} &\geq z_{n,k-1} + T\_\mathrm{fur} \\ 1 \leq z_{n,k} &\leq T - T\_\mathrm{fur}. \end{aligned} \tag{33}$$

IV. Dispacthing Potential Evaluation Model of Purchased Power Load

Combining the scheduling of multienergy system and the concomitant energy change caused by production process optimization, the dispatching potential evaluation of purchased power load for an ISP belongs to a mathematical programming problem.

All the above modeling of multienergy system and adjustable production processes is integrated together via the electrical power balance, described as (34)

$$\begin{aligned} & P_t^{\mathrm{gen,gas}} + P_t^{\mathrm{gen,heat}} + P_t^{\mathrm{gen,PV}} + P_t^{\mathrm{grid}} \\ & = P_t^{\mathrm{roll}} + P_t^{\mathrm{fur}} + P_t^{\mathrm{oxy}} + P_t^{\mathrm{nit}} + P_t^{\mathrm{other}}. \end{aligned} \tag{34}$$

Since the interaction between power supply and demand has different situations, like peak cutting, valley filling, reserve service, and emergency demand response, the dispatching potential has different forms. Here, we take peak power cutting potential of an ISP as an example. The adjustment amount of purchased power based on its baseline operation level can be described as (35)

$$P_t^{\mathrm{change}} = P_t^{\mathrm{grid,base}} - P_t^{\mathrm{gridt}} \in T^{DR}. \tag{35}$$

For the intension to evaluate the dispatching potential of ISP purchased power, two dimensions describing the potential need to be figured out: 1) the maximum adjustable potential value of each moment during scheduled dispatching period; 2) the duration evaluation of the maximum potential. Thus, two objective functions are proposed here for each dimension, formulated as follows.

A. Maximum Dispatching Potential Evaluation Model

To evaluate the maximum peak load cutting value of an ISP during required scheduling time, the objective function can be formulated as (36), subjected to the coupling multienergy system and related production process constraints (1)–(35) constructed in Sections II and III

$$\begin{aligned} & \max_{t \in T^{DR}} P_t^{\mathrm{change}} \\ & s.t. \; (1) - (34) \,. \end{aligned} \tag{36}$$

B. Maximum Dispatching Potential and Its Duration Evaluation Model

Current energy markets with the participation of demand side generally require all the entities to supply both the adjustable capacity and duration of dispatching resources for market access. This is of great important for ISOs or dispatch sectors to make economic dispatch schedule. However, technically, it is difficult to evaluate the maximum potential and its duration time of an ISP with one-shot optimization method. To tackle this problem, a maximum dispatching evaluation model with fixed step-size duration is proposed here. With the same objective function (36), a group of constraints needs to be considered into the model of the previous subsection, denoted as (37)

$$P_{t+i}^{\text{change}} \geq P_t^{\text{change}}, i = 1, 2, \ldots, \frac{\Delta T^{\text{dur}}}{\Delta t}. \tag{37}$$

As expressed in (37), the cutting load must be higher that the maximum cutting load at moment t [the objective function of (36)] within a given duration ΔT^{dur}. Once (37) is added to model (36), the model can evaluate the maximum potential with a minimum duration ΔT^{dur}. With the adjustment of ΔT^{dur} with a fixed step size (set as 15 min in our case study), the relationship between maximum potential and its duration can be evaluated at moment t. Such that the entities of ISPs can join different demand response projects and auxiliary markets, according to the potential and duration evaluation.

C. Solving Methods of the Proposed Model

Mathematically, the dispatching potential evaluation model proposed is a MILP, can be solved with several mature solvers. In this article, the optimization was solved with CPLEX solver.

V. Case Study

A. Case Setting

Case study is based on an actual ISP in Jiangsu Province. The plant has five identical gas turbines, one CDQ waste heat turbine, and two electric arc furnaces EAFs. The dispatching potential evaluation models shown above are solved in MATLAB with CPLEX solver.

Several cases are designed here to check the performance of the proposed evaluation method in different load scheduling potential assessment models compared to the normal case with realistic running data (Origin). All the cases are supposed to evaluate the dispatching potential to attend the peak cutting demand response during 10:00–12:00. Three cases are listed as follows.

Case 1: Purchased power only with multienergy system scheduling.

Case 2: Purchased power only with production processes scheduling.

Case 3: Purchased power with combined multienergy system energy and production processes scheduling proposed in this article.

To prove the efficiency of our proposed method to evaluate the maximum potential and its duration, two subcases are set to the above three cases, respectively. The two subcases are denoted as Case A and B.

Case A: The maximum adjustable potential of purchased power is evaluated without considering its duration by solving model (36). In order to evaluate the maximum potential under different adjustable resources, these cases are denoted as Case 1.A, Case 2.A, and Case 3.A.

Case B: The maximum adjustable potential of purchased power is evaluated considering its duration by solving model consist of (36) and (37). Similarly, to evaluate the maximum potential and its potential under different adjustable resources, Case 1.B, Case 2.B, and Case 3.B are designed. In addition, to show the different potential with different adjustable resources at different moments, we set Case 1.B.I, Case 2.B.I, and Case 3.B.I for moment 10:00 and Case 1.B.II, Case 2.B.II, and Case 3.B.II for moment 12:00.

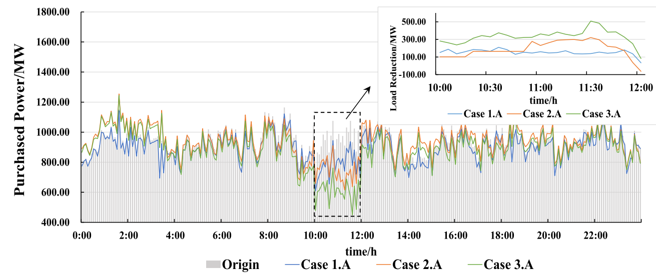

Fig. 4. Load curves in different cases.

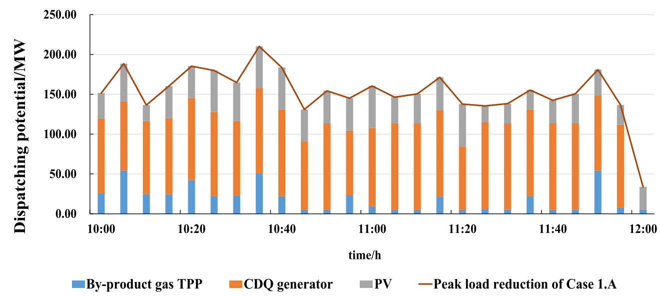

Fig. 5. Maximum dispatching potential contributed by energy-system adjustment in Case 1.A.

B. Analysis on Maximum Dispatching Potential

With the objective function of maximum value of purchased power dispatching potential, the goal in (36), the results of previously defined three cases are denoted as Case 1.A, Case 2.A, and Case 3.A separately. Fig. 4 shows the purchased power load and maximum dispatching potential of different cases.

As shown in Fig. 4, when energy optimization and process optimization are respectively considered, the load decreases during the time of demand response project, the average decrease of power purchase is about 10.6% and 8.8% of “Origin,” and the maximum dispatching potential is 15.76% and 16.8%, respectively. In the case of joint optimization (Case 3.A), the load was reduced to a greater extent, with an average decrease of 19.5% and a maximum decrease of 29.4%.

According to the above data, the average dispatching potential in Case 3.A is approximately equal to the sum of Case 1.A and Case 2.A, while the maximum dispatching potential is less than the sum of them, because the maximum dispatching potential occurs at different times.

According to Figs. 5 and 6, what can be analyzed is as follows. In Case 1.A, the maximum dispatching potential is consisted of by-product gas TPP, CDQ power generation, and PV power generation.

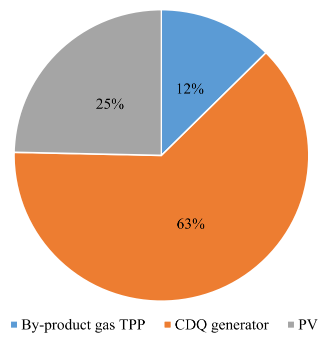

Fig. 6. Pie chart of dispatching potential contributed by energy-system adjustment in Case 1.A.

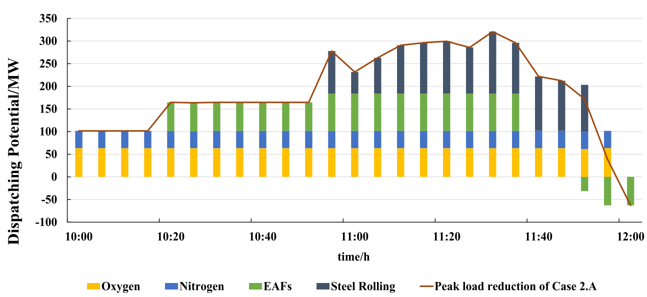

Fig. 7. Maximum dispatching potential contributed by production-process adjustment in Case 2.A.

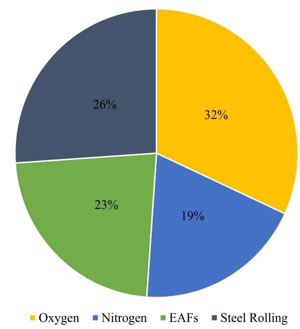

Fig. 8. Pie chart of dispatching potential contributed by production-process adjustment in Case 2.A.

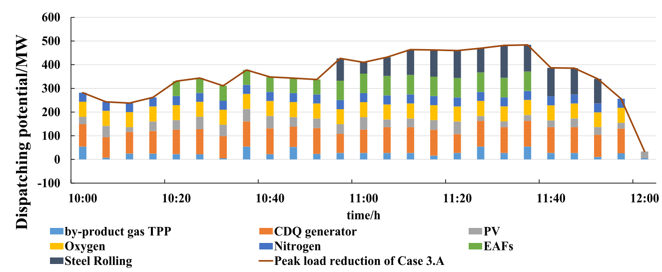

Fig. 9. Maximum dispatching potential contributed by joint energy-system and production-process adjustment in Case 3.A.

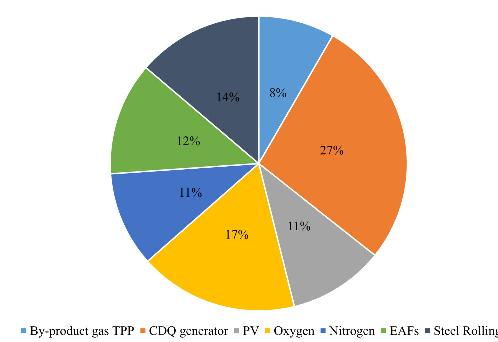

Fig. 10. Pie chart of dispatching potential contributed by joint energy-system and production-process adjustment in Case 3.A.

In this calculation example, the maximum allowable variation of gas holders and other relevant constraints are set relatively small, so the power generation of by-product gas is a bit small.

Obviously, as only the integrated energy system is invoked in this case, interruptible and transferrable production loads are not involved, so the scheduling potential has little difference in different time periods. Although there is no significant large amount of dispatching potential in most time during 10:00–12:00, negative potential optimization never happens. That is the difference between Case 1.A and the next two cases.

In this case, maximum dispatching potential is mainly composed of three production processes in this case: air separation system, steel rolling production line, and electric arc furnaces. Among them, the air separation system produces oxygen and nitrogen, this system and electric arc furnaces are transferable load, and the steel rolling line is interruptible load.

According to Fig. 7 and Fig. 8, first of all, it is important to point out that positive values in the figure indicate a contribution to maximum dispatching potential, while negative values indicate the opposite. It is obvious that negative potential scheduling occurs in the electric arc furnaces at the end of the scheduling period. That is because the limited load translation capacity of the electric arc furnaces makes it impossible to transfer all the loads out of the scheduling period.

In addition, it can be seen that the interruption of the rolling line occurs between 10:55 and 11:50, which provides a greater maximum dispatching potential for the system and compensates for the shortcomings of the electric arc furnaces.

In general, the contribution proportion to maximum dispatching potential of the four parts in Case 2.A is similar, and the negative potential scheduling has small impact to the system. The overall optimization performance is acceptable.

When it comes to the result of Case 3.A, shown as Fig. 9 and Fig. 10, the first should be pointed out is that the maximum dispatching potential is much more than Case 1.A and Case 2.A.While its volatility is more severe than the first two cases, and negative scheduling potential does not occur in the end part of the scheduling period. This means that the energy system makes up for the lack of schedulable potential of the system.

In conclusion, compared with the results of Case 1.A and Case 2.A separately, the dispatching potential of Case 3.A is significantly improved with joint optimization of energy system and production processes. the maximum schedulable potential of purchase power in Case 3.1 reached to about 500 MW, that is

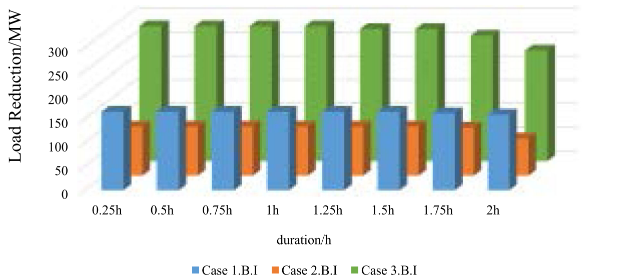

Fig. 11. Maximum dispatching potential with different duration in different cases.

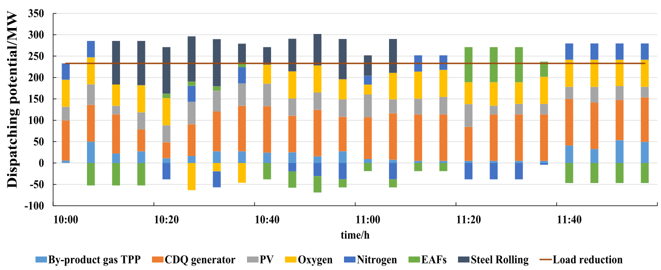

Fig. 12. Purchased power maximum dispatching potential contributed by joint energy-system and production-process adjustments in Case 3.B.I.

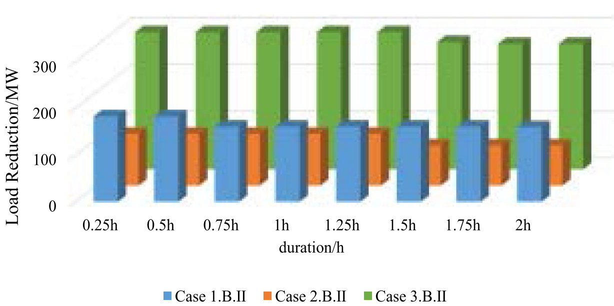

Fig. 13. Maximum dispatching potential with different duration in different cases.

150% higher than that of Case 1.A and 54% higher than that of Case 2.A.

The necessity of combined energy and production optimization can be proved in this case according to exploiting the dispatching potential of purchased power in ISPs.

C. Analysis on Maximum Dispatching Potential and Duration

In order to meet the demand of maximum dispatching potential for power grid, it is necessary to research the maximum dispatching potential with different duration in different cases that iron and steel enterprises can provide in a certain time period. By solving the proposed maximum dispatching evaluation model with fixed step-size duration with (37), the relationship between maximum potential and its duration can be obtained in different case, denoted as Case 1.B, Case 2.B, and Case 3.B. Fixed step size of duration is set to 0.25 h.

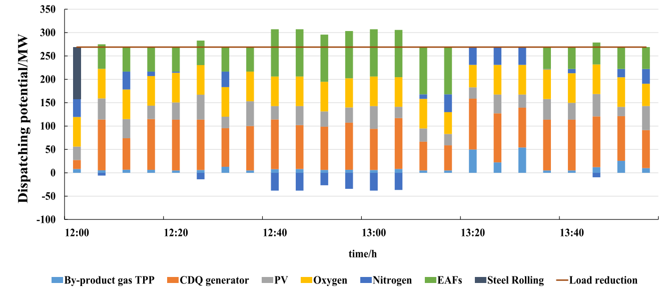

Fig. 14. Purchased power maximum dispatching potential contributed by joint energy-system and production-process adjustments in Case 3.B.II.

TABLE I
MAXIMUM DISPATCHING POTENTIAL WITH DIFFERENT DURATION IN DIFFERENT CASES

	0.25h	0.5h	0.75h	1h	1.25h	1.5h	1.75h	2h
Case 1.B.I	165	165	165	165	165	165	162	159
Case 2.B.I	103	103	103	103	103	103	101	78
Case 3.B.I	284	284	284	284	278	278	264	233

TABLE II
MAXIMUM DISPATCHING POTENTIAL WITH DIFFERENT DURATION IN DIFFERENT CASES

	0.25h	0.5h	0.75h	1h	1.25h	1.5h	1.75h	2h
Case 1.B.II	183	183	161	161	161	161	161	160
Case 2.B.II	111	111	111	111	111	86	86	86
Case 3.B.II	294	294	294	294	294	273	269	269

To illustrate different relationship of maximum value and duration at different moment, two cases are set here: set one moment as 10:00 and the other is 12:00. Both of the cases are conducted with duration evaluation taking (37) into account.

1) Result of Case I: Table I and Fig. 11 show maximum dispatching potential and its duration under different conditions at 10:00.

It can be seen that Case 3.B has the strongest ability to reduce load, while that of Case 2.B is the weakest. It is worth noting that maximum dispatching potential does not decrease with the increase of time when the scheduling period is less than 1 h. That is because the system is constrained by the change rate of the capacity of gas holders, the amount of electricity generated, etc., so it cannot provide greater maximum dispatching potential in a short period of time.

With the further increase of the duration of maximum dispatching potential, the maximum dispatching potential gradually decreases, which reflects the lack of long-term scheduling ability of the system.

Fig. 12 shows maximum dispatching potential contributed by different energy-system and production-process adjustments when the maximum dispatching potential lasts for 2 h.

2) Result of Case II: Table II and Fig. 13 show maximum dispatching potential and its duration under different conditions at 12:00. Similarly, maximum dispatching potential does not decrease with the increase of duration when the scheduling period is less than 1 h. But Case 1.B.II is an exception. It fell between 0.5 and 0.75 h. This is because of the increased demand for gas during this period and the reduction of PV output.

Fig. 14 shows maximum dispatching potential contributed by different energy-system and production-process adjustments when the maximum dispatching potential lasts for 2 h.

It can be seen that the maximum dispatching potential in this case is slightly greater than the Case I, showing that the dispatching potential is different at different moments. Besides, the contributions to dispatching potential of different adjustable resources are also differed at different moments.

V. Conclusion

ISPs have significant potential to participate in the interaction with power supply. Based on the multienergy system modeling, as well as the modeling of adjustable production processes, the maximum dispatching potential of outsourcing power in an ISP was quantified by the established evaluation method. To study the relationship of maximum dispatching potential and its duration, a fixed-step duration evaluation method was proposed as an MILP problem. Numerical result shown the outstanding contribution to dispatching potential for ISPs to take production process optimization into consideration without affecting the productivity.

References

[1] X. Lu *et al.*, "The relationship between energy consumption and CO_2 emission reduction in iron and steel plants [J]," *J. Univ. Sci. Technol. Beijing*, vol. 34, no. 12, pp. 1445–1452, 2012.

[2] Q. Zhang *et al.*, "Coupling model of surplus gas, steam and power in iron and steel plants and its application [J]," *CIESC J.*, vol. 62, no. 3, pp. 753–758, 2011.

[3] G. Li *et al.*, "Optimal operation scheduling of large-scale steam pipe network [J]," *Chem. Eng. Prog.*, vol. 1, pp. 77–81, 2007.

[4] Q. Zhang *et al.*, "Coupling optimization and application of gas, steam and power system in iron and steel plants [J]," *CIESC J.*, vol. 69, no. 7, pp. 3149–3158, 2018.

[5] X. Xia *et al.*, "Gas scheduling based generation dispatching of self-provided power plants for energy-intensive plants [J]," *Power Syst. Automat.*, vol. 40, no. 22, pp. 160–167, 2016.

[6] Q. Shi *et al.*, "Short-cycle optimization scheduling model of by-product gas in iron and steel plants [J]," *Iron Steel*, vol. 51, no. 8, pp. 81–89, 2016.

[7] X. Zhao *et al.*, "Optimal scheduling of a byproduct gas system in a steel plant considering time-of-use electricity pricing [J]," *Appl. Energy*, vol. 195, pp. 100–113, 2017.

[8] X. Zhao *et al.*, "A MILP model concerning the optimisation of penalty factors for the short-term distribution of byproduct gases produced in the iron and steel making process [J]," *Appl. Energy*, vol. 148, pp. 142–158, 2015.

[9] J. Zhao, C. Sheng, W. Wang, W. Pedrycz, and Q. Liu, "Data-based predictive optimization for byproduct gas system in steel industry [J]," *IEEE Trans. Automat. Sci. Eng.*, vol. 14, no. 4, pp. 1761–1770, Oct. 2017.

[10] T. Wang *et al.*, "Evolutionary adaptive dynamic programming algorithm for converter gas scheduling of steel industry [C]," in *Proc. 6th Int. Symp. Adv. Control Ind. Processes*, Taipei, Taiwan, 2017, pp. 137–142.

[11] S. G. J. van Niekerk, W. J. J. Breytenbach, and J. H. Marais, "Developing an optimisation model for industrial furnace gaseous fuel distribution for energy cost savings [C]," in *Proc. Int. Conf. Ind. Commercial Use Energy*, Cape Town, South Africa, 2017, pp. 1–4.

[12] L. Gan *et al.*, "A method to evaluate the power dispatching potential of energy intensive steel enterprises [C]," in *Proc. IEEE/IAS Ind. Commercial Power Syst. Asia*, Weihai, China, 2020, pp. 290–295.

[13] T. Li and Z. Su, "Two-stage genetic algorithm for production scheduling problem of steelmaking and continuous casting [J]," *Chin. J. Manage. Sci.*, vol. 17, no. 5, pp. 68–74, 2009.

[14] S. Jiang *et al.*, "A bi-layer optimization approach for a hybrid flow shop scheduling problem involving controllable processing times in the steelmaking industry [J]," *Comput. Ind. Eng.*, vol. 87, pp. 518–531, 2015.

[15] M. Tan*et al.*, "A two-stage optimization of hot rolling batch scheduling for economic load dispatch under time-of-use electricity tariffs [J]," *J. Central South University Science Technology*. vol. 45, no. 10, pp. 3456–3462, 2014.

[16] D. Sun, "The configuration and process selection of air separation equipment in iron and steel plant construction [J]," *Cryogenic Technol.*, vol. 5, pp. 8–12, 2007.

[17] J. Hao *et al.*, "A soft-decision based two-layered scheduling approach for uncertain steelmaking-continuous casting process[J]," *Eur. J. Oper. Res.*, vol. 244, no. 3, pp. 966–979, 2015.

[18] S. Lin *et al.*, "Genetic algorithm based on duality principle for bilevel programming problem in steel-making production [J]," *Chin. J. Chem. Eng.*, vol. 22, no. 7, pp. 742–747, 2014.

[19] S. Mitra, J. Pinto, and I. Grossmann, "Optimal multi-scale capacity planning for power-intensive continuous processes under time-sensitive electricity prices and demand uncertainty. Part I: Modeling [J]," *Comput. Chem. Eng.*, vol. 65, pp. 89–101, 2014.

[20] A. Hasanbeigi, M. Arens, and L. Price, "Alternative emerging ironmaking technologies for energy-efficiency and carbon dioxide emissions reduction: A technical review [J]," *Renewable Sustain. Energy Rev.*, vol. 33, pp. 645–658, 2014.

[21] W. Sun *et al.*, "Material and energy flows of the iron and steel industry: Status quo, challenges and perspectives [J]," *Appl. Energy*, vol. 268, 2020, Art. no. 114946.

[22] H. Hadera *et al.*, "Optimization of steel production scheduling with complex time-sensitive electricity cost [J]," *Comput. Chem. Eng.*, vol. 76, pp. 117–136, 2015.

[23] Z. Han, J. Zhao, and W. Wang, "An optimized oxygen system scheduling with electricity cost consideration in steel industry [J]," *IEEE/CAA J. Automatica Sinica*, vol. 4, no. 2, pp. 216–222, Apr. 2017.

[24] M. F. Torquato, G. Martínez-Ayuso, A. A. Fahmy, and J. Sienz, "Multi-objective optimization of electric arc furnace using the non-dominated sorting genetic algorithm II [J]," *IEEE Access*, vol. 9, pp. 149715–149731, 2021.

[25] T. Yang, L. Gan, X. Chen, G. Li, and K. Yu, "Dispatching potential evaluation of purchased power load in iron and steel plant considering production process optimization [C]," in *Proc. IEEE/IAS Ind. Commercial Power Syst. Asia*, Chengdu, China, 2021, pp. 1252–1255.

[26] H. Li, Z. Wang, and J. Zhou, "Energy saving calculation and analysis of independent coking dry quenching coking waste heat power generation project [J]," *Henan Chem. Ind.*, vol. 37, no. 10, pp. 29–32, 2020.

[27] S. Liu *et al.*, "Optimization strategy of production load flattening in large industrial enterprises [J]," *J. Power Syst. Automat.* (in Chinese), vol. 29, no. 10, pp. 138–144, 2017.

[28] Y. Zhang, J. Zhou, and G. Zhai, "Energy consumption analysis and economic operation of large-scale air separation in iron and steel plants [J]," *Metallurgical Energy*, vol. 33, no. 5, pp. 6–8, 2014.

Lei Gan (Member, IEEE) was born in Jiangsu Province, China. He received the B.S. and Ph.D. degrees from North China Electricity Power University (NCEPU), Beijing, China, in 2010, and 2017, respectively, both in electrical engineering.

Since 2017, he has been with the College of Energy and Electrical Engineering, Hohai University, Nanjing, China, where he is currently a Lecturer and Postdoctor. His research interests include power system planning and operation and integrated energy system operation.

Tianyu Yang was born in Jiangsu Province, China. He is currently working toward the B.S. degree in electrical engineering and automation from the College of Energy and Electrical Engineering, Hohai University, Nanjing, China.

His research interests include interaction between energy supply and demand and integrated energy system operation.

Xingying Chen (Senior Member, IEEE) was born in Wuxi, China. She received the B.Eng. degree from Southeast University, Nanjing, China, in 1984, the M.Eng. degree from Hohai University, Nanjing, China, in 1995, and the Ph.D. degree from Southeast University, in 2002, all in electrical engineering.

She joined the Faculty of Hohai University, Nanjing, China, in 1984, and has been a Professor there since 2002. Her research interests include distribution and utilization system of electric power, power market, energy management and control, and energy economics.

Gengyin Li (Member, IEEE) was born in Hebei Province, China. He received the B.S., M.S., and Ph.D. degrees from North China Electricity Power University (NCEPU), Beijing, China, in 1984, 1987, and 1996, respectively, all in electrical engineering.

Since 1987, he has been with the School of Electrical and Electronic Engineering, NCEPU, where he is currently a Professor and Executive Vice Dean. His research interests include power system analysis and reliability, power systems economics, power quality analysis and control, and HVdc and VSC-HVdc transmission technology.

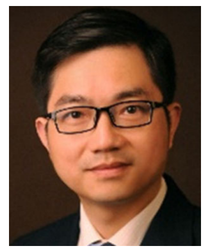

Kun Yu (Member, IEEE) was born in Chongqing, China. He received the B.Eng. and M.Eng. degrees from Hohai University, Nanjing, China, in 2000 and 2003, respectively, and the Ph.D. degree from Zhejiang University, Hangzhou, China, in 2011, all in electrical engineering.

Since 2003, he has been an Associate Professor with Hohai University. His research interests include self-healing control and optimal dispatching of smart distribution grid, power distribution and utilization system multienergy complementary, and efficient operation.